Solder Metalization Interdiffusion in Microelectronic Interconnects

Zribi, R.R. Chromik, R. Preshus, J. Clum, K. Teed, L. Zavalij, J. DeVita, J. Tova, E.J. Cotts
State University of New York at Binghamton—Physics Department
P.O. Box 6016
Binghamton, NY 13902
ecotts@binghamton.edu

Abstract

We investigated the growth of intermetallic compounds in Cu/Ni/Au/PbSn solder joints, and the effect of these compounds on the mechanical integrity of the joints. The substrates which we investigated had been Au plated by one of three different techniques, with Au finish thicknesses ranging from 0.02 to 2.6 μm. After solder reflow, the solder joints were annealed in an inert atmosphere at a temperature of 150 ^{o}C, for up to 1000 h. Tensile-shear stress tests were performed on solder joints after different annealing times. Two distinct failure mechanisms were observed, the first (always observed in as-reflowed joints) was termed ductile, and was associated with failure within the solder ball. In solder joints with thicker layers of Au plating, a brittle failure mechanism, which reflected a factor of two decrease in joint toughness, was observed after thermal aging. Structural examinations using optical and electron microscopy of cross sectioned solder joints revealed the growth of Ni_3Sn_4 at the solder/Ni interface after reflow. After thermal aging of solder joints with thicker layers of Au plating, we observed the further growth of $(Au_{0.5}Ni_{0.5})Sn_4$ at the Ni_3Sn_4/solder interface. The appearance of this ternary alloy, which has the same structure as $AuSn_4$, was correlated with the decrease in toughness of the solder joints.

Introduction

The formation of intermetallic compounds (IC's) has always concerned engineers and scientists who are involved in the design of metallic structures. These compounds often are found to be brittle at low temperatures and therefore are a potential cause of failure of solder devices. Electronic packaging is an area where severe embrittlement problems related to IC's continue to arise.

A number of different IC's have been identified as the cause of failures in electronic packages. For instance, $AuSn_4$ is particularly well known for its deleterious effect on the mechanical reliability of solder joints. This binary Au-Sn intermetallic is a weak, brittle compound that degrades the thermal fatigue life of the joint when present in high concentrations in PbSn solder[5]. A large range of Au concentrations in PbSn solder have been explored by several investigators [3,4,5]. In these cases, $AuSn_4$ was observed as a precipitate, spread throughout the solder. According to these works, Au has a propensity to embrittle solder joints when present in a range of concentrations that extends from 2 to 7 wt%. Other investigators [1] stated that as a rule of thumb, Au concentrations of greater than 3 wt% in a PbSn solder joint cause considerable degradation. The present work concerns a failure mechanism due to a ternary Au IC which manifests itself for Au concentrations as low as 0.2 wt%.

A specific example of the detrimental effect of Au on solder joints concerns premature mechanical failures in ball grid array (BGA) Cu/Ni/Au/PbSn solder joints [1]. In these BGA's, Au is used to protect Ni from corrosion, before reflow. Au has a high solubility in molten solder, and during reflow it dissolves quickly into the molten solder [2,3,4]. The final solder joint microstructure and composition depend upon the initial thickness of Au, the reflow profile and the thermal aging of the sample. Nevertheless, a number of investigations [1,5] have reported the formation of a $AuSn_4$ intermetallic near the Ni/solder interface. In publication [1], the authors found that $AuSn_4$ nucleated in the PbSn solder after reflow. The authors reported that upon thermal aging at 150 ^{o}C, this $AuSn_4$ migrated from the bulk of the solder joint to the solder interface adjacent to the Ni_3Sn_4 intermetallic. These investigators reported a detrimental effect of the $AuSn_4$ on the bending strength of BGA assemblies, with breakage energies dropping considerably. The coexistence of these two phases, with poor adhesion properties to each other, was held to be responsible for the observed deterioration of the joint. The mechanism driving the migration of the $AuSn_4$ alloy at the Ni_3Sn_4/solder interface has not previously been elucidated.

We conducted our investigation in an attempt to understand the mechanism driving the formation of Au IC's at the Ni_3Sn_4/solder interface during thermal aging of Cu/Ni/Au/solder BGA's. Different substrates from two different vendors, with three Au/Ni plating categories (electrolytic, immersion and selective) were used to prepare the BGA packages. We examined the effect of thermal aging on the toughness and the ductility of the joints. Consistent with prevoius results, we observed the growth of a Au IC at the Ni_3Sn_4/solder interface during thermal aging at intermediate temperatures (e.g. 150 ^{o}C). We found that the concentration of Au in the joint is important , since it dictates how thick an IC can possibly grow. In our case, the Au IC was identified to be a ternary Au-Ni-Sn alloy, approximately $Au_{0.5}Ni_{0.5}Sn_4$.

Samples preparation

FR4 substrates from two different vendors were used to make the specimens for this study. The printed circuit boards were populated with eutectic solder spheres arranged in one row around the perimeter of the board layout. After placing the balls with a placement machine, the boards were sent to a reflow oven. The reflow procedure is carried out according to vendor recommendations and the reflow profile is displayed in **Figure 1**.

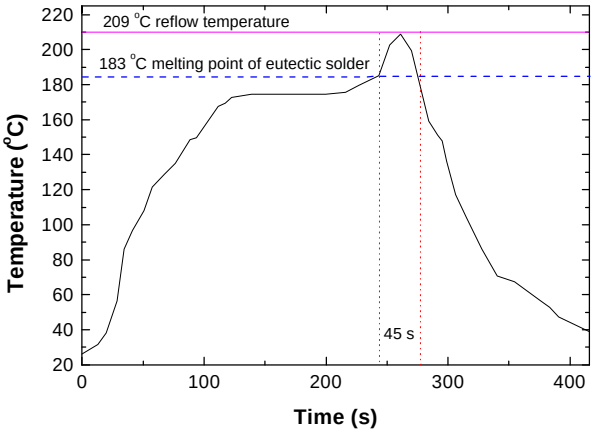

Figure 1: Temperature-reflow profile.

The samples were subsequently sealed in argon and annealed in a convection oven at 150°C for up to 1000 h. After annealing, the samples were cross-sectioned and prepared for inspection.

I. Equilibrium Phase diagram analysis

A. Dissolution of Au and Ni in molten solder

When eutectic Sn-Pb solder is reflowed on Ni/Au-coated copper pads, interfacial dissolution reactions occur. This dissolution is controlled mainly by three parameters: temperature, solubility of the solute at the operating temperature, and its initial concentration. These parameters, together with experimental measurements, provided sufficient data for an estimate of the dissolution rate of Au and Ni in molten solder during reflow.

A published paper [2] established that dissolution rates of both Ni and Au in eutectic PbSn solder follow an Arrhenius relationship. Although the investigation used thin wires of Ni and Au in a rather large volume of molten solder, the paper reported good agreement with similar data obtained for thin films. By extrapolating the data provided in [2] towards lower temperatures (**Figure 2)**, both Ni and Au dissolution rates were estimated to (R_{Ni}=0.002 µm/s and R_{Au}=1.33 µm/s) at 209°C (the reflow temperature in our case).

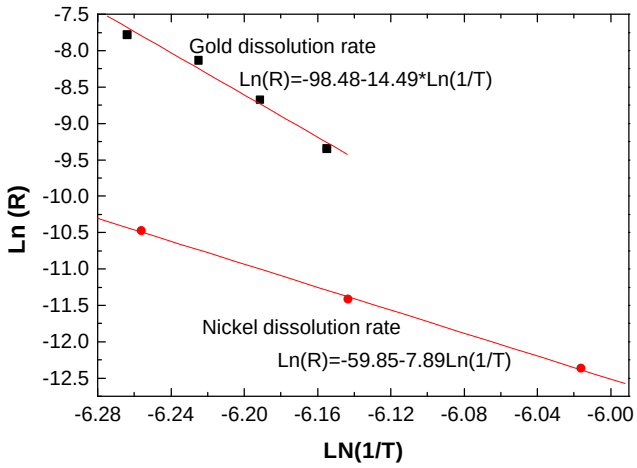

Figure 2: Dissolution rate of Au/Ni in eutectic solder versus temperature.

Figure 3 and Figure 4 show sections of the ternary phase diagrams of Pb-Sn-Au and Pb-Sn-Ni respectively. From these diagrams the solubility limit of Au and Ni in the molten eutectic solder are estimated to 3-4 at % for Au and about 10^{-5} at % for Ni.

As the dissolution rate of Au exceeds that of Ni by almost three orders of magnitude, and the solubility of Au that of Ni by five orders of magnitude, the thin Au layer is expected to disappear relatively quickly during reflow, exposing Ni for quite a long time to the action of the molten solder

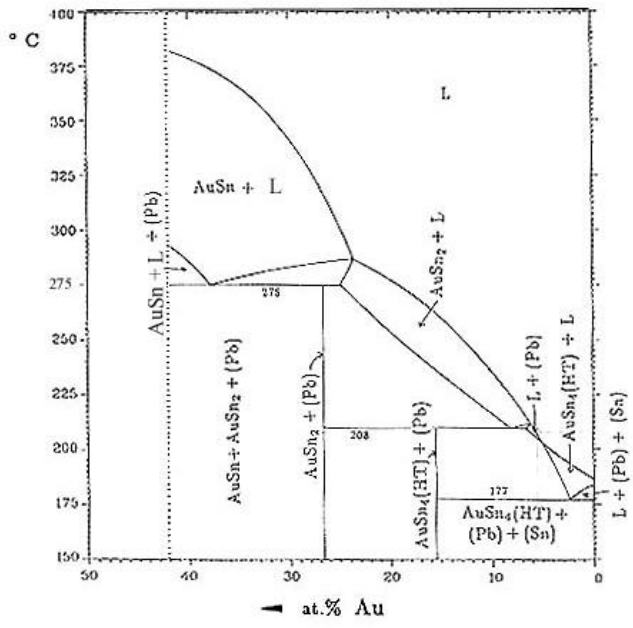

Figure 3: Binary section of the ternary phase diagram Au-Sn-Pb.

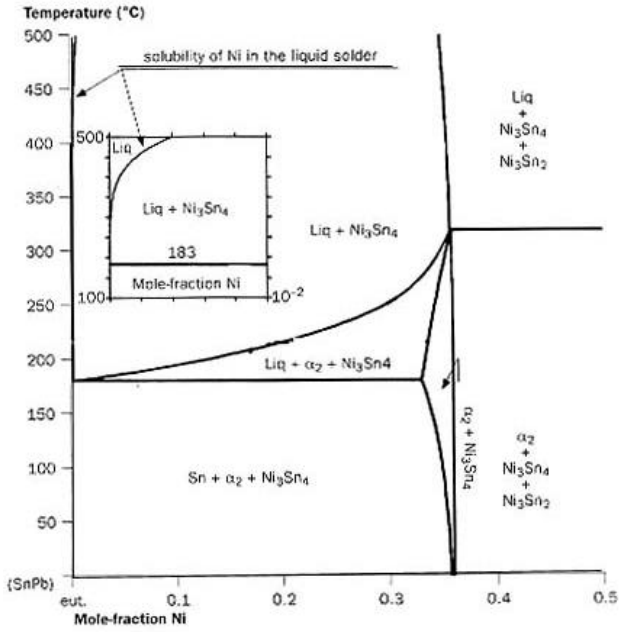

Figure 4: Binary section of the ternary phase diagram Ni-Sn-Pb.

In order to determine the thicknesses of the Au and Ni layers for the three plating categories, a Scanning Auger Microprobe was used to analyze a 60μm x 50μm area on each pad with a 3 keV electron beam. The surface was exposed to series of five 1-minute sputters (with 3 keV Ar ions at a rate of 0.07 nm/s), separated by surface scans. The resulting concentration profiles of the detected elements were plotted in concentration versus depth curves. The Au and Ni layer thicknesses are reported in **Table 1**.

Sample	Electrolytic (1)	Electrolytic (2)	Immersion	Selective
Au thickness (μm)	2.6	0.75	0.25	0.02

Table 1: Measured thicknesses of the Au and Ni layers for different plating technologies.

Assuming that the molten solder perfectly wets the Au surface, and using the dissolution rate of 1.3 μm/s, it would take less than a second (0.5 s) to dissolve the thickest layer of Au (electrolytic). The concentrations of Au and Ni in molten solder, given in **Table 2**, are estimated based upon the average dimensions of the BGA solder balls measured by a calliper. Within the time afforded by the reflow process, the Ni-layer will therefore be exposed to the molten solder for approximately 35 s. This time accounts for the wetting time, which would be approximately 10 s [6].

at % (in molten solder)	Au	Ni (less than)
Electrolytic 1	0.34	10^{-5}
Electrolytic 2	0.1	10^{-5}
Immersion	0.031	10^{-5}
Selective	0.0027	10^{-5}

Table 2: Concentrations of Au and Ni in the molten solder.

The Ni dissolution process will continue until the liquid solder saturates. At this time, the most Sn-rich intermetallic compound precipitates and grows. In agreement with the binary section of the ternary phase diagram Pb-Sn-Ni (**Figure 4**), the precipitating intermetallic is Ni_3Sn_4. The nucleation of this phase occurs at the Ni/solder interface.

Given the extremely low solubility limit of Ni in molten eutectic solder and the dimensions of the BGA spheres, a layer of Ni of only 0.0048 μm is expected to dissolve before the formation of Ni_3Sn_4. (**Figure 5**). During most of the reflow time Ni_3Sn_4 will be growing. The phase growth naturally involves both liquid and solid state reactions as the eutectic is kept in a liquid state and the emerging solid phase is adjacent to the solid layer of Ni. The reaction constant for the solid/liquid state reaction between Ni and Sn is estimated to 3.2×10^{-10} cm^2/s at 209°C [7]. Therefore, a Ni_3Sn_4 intermetallic layer of approximately 1μm in thickness is expected to grow at the interface during reflow.

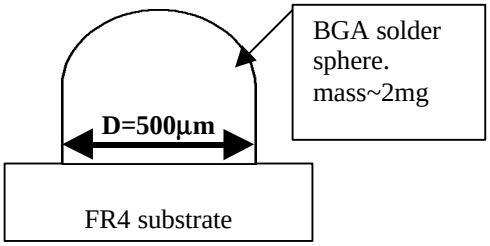

Figure 5: Geometrical configuration of a typical sample.

B. Crystallization Analysis

We examine the changes which occur for a single, homogeneous Au-Sn-Pb fluid under equilibrium conditions. Although our samples were rapidly cooled from the melt, consideration of equilibrium crystallization paths provides some illumination of actual processes. The average concentrations of Au, Pb and Sn in the solder balls are estimated in **Table 3** for the three types of Au plating. During solder reflow, Au remains in solution with Sn. Considering the very low Au solubility in the Pb-rich phase of the solder, most of the dissolved Au is expected to be found in the Sn-rich phase.

Sample	Electrolytic (1)	Electrolytic (2)	Immersion	Selective
at % Au	0.34	0.1	0.031	0.0027
at % Sn	74.4	74.58	74.6	74.7
at % Pb	25.26	25.32	25.37	25.29

Table 3: Atomic concentration of Au, Sn and Pb in molten solder before cooling.

We begin by assuming a homogeneous solder melt [2,4]. Upon cooling, the first solid crystallizes after the temperature goes slightly below the liquidus temperature. As the arrows on the phase diagram shown in **Figure 6** point to falling temperatures, the crystallization path starting at the initial compositions will terminate at the eutectic E_2.

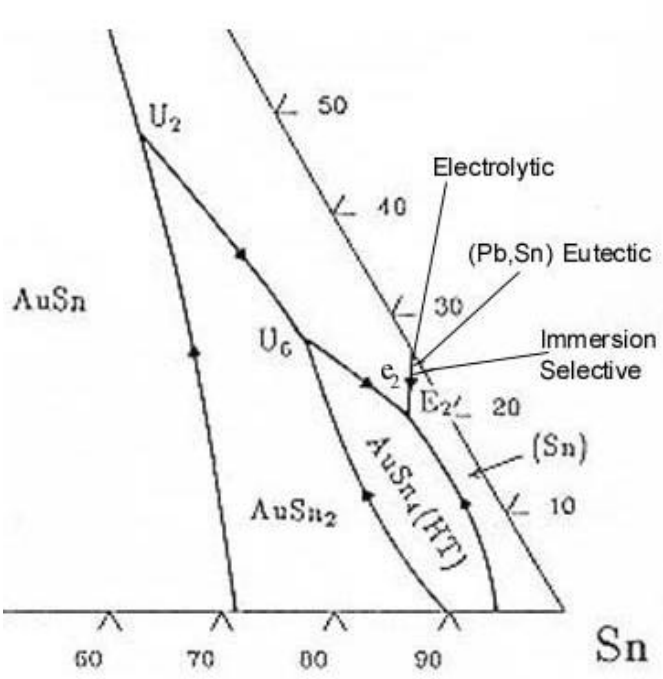

Figure 6: Liquidus projection of the ternary phase diagram.

The initial composition of the solution falls in the Sn primary crystallization field for all our samples, as shown in **Figure 6**. Therefore, the first solid to form from the melt is a Sn-rich phase. This Sn depletion might yield a typical flower shaped morphology of the solidifying phase.

As the temperature of the system declines along the boundary line e_2-E_2, eutectic solder continues to solidify and hence the remaining liquid gets enriched in Au regardless of the sample category. This process will continue until the eutectic temperature T_{E2}=176°C is reached. Eventually, below the eutectic temperature, the material is completely solid as a result of the eutectic reaction:

$$E_2: L \Leftrightarrow AuSn_4(HT)+(Pb)+(Sn)$$

The indication is that when the initial liquid compositions in Au are homogeneous, $AuSn_4$ will only nucleate if equilibrium conditions are fulfilled throughout the cooling process. Such conditions require a slow cooling rate, which is not provided in our experiments. Consequently $AuSn_4$ is not likely to form in any appreciable amount after reflow in our samples.

II. Phase identification and intermetallic growth mechanisms

Optical and electron metallography were used to examine cross-sectioned samples. One of the objectives was to determine the effect of thermal aging on the microstructure. Thus, all samples were aged at 150°C for 0.5 h, 1 h, 4 h, 9 h, 40 h, 150 h, 450 h and examined together with unaged specimens.

Five distinct phases were commonly observed in all samples, regardless of the aging time. These phases were identified by EDS (Energy Dispersive Spectroscopy) spectra, along with their spatial location in the sample, to be Cu, Ni, Ni_3Sn_4, and the Sn-rich and the lead-rich phases of the solder, as shown in **Figure 7**.

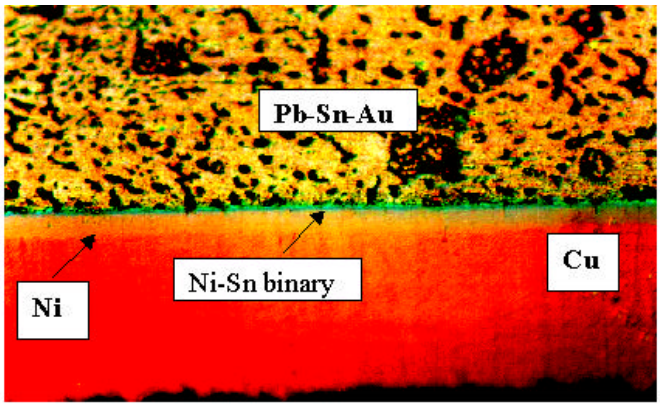

Figure 7: Optical micrograph 1000X. Interfacial microstructure of an as-reflowed joint.

During thermal aging at 150 °C, the interfacial Ni_3Sn_4 phase grows somewhat thicker. In some instances, a Ni-Au-Sn ternary phase was observed to grow in addition to this binary Ni-Sn phase. Continual growth of this phase as a function of annealing time was observed for the electrolytic samples. This manifest phase showed up in the immersion samples as well, but only after 450 h of annealing at 150°C.

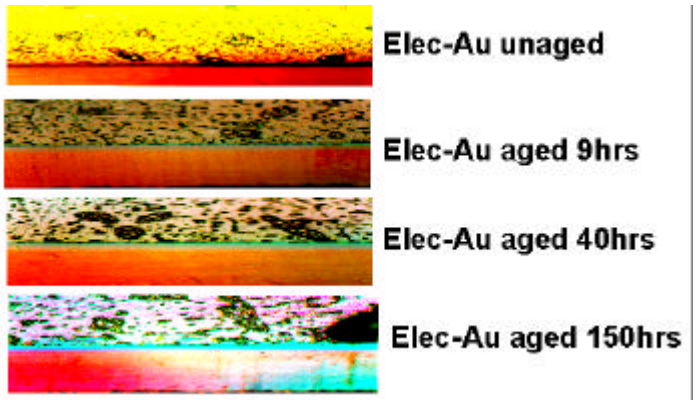

Figure 8: Optical micrograph (1000X). Ni-Sn intermetallic growth at the interface solder-Ni.

The thickness of the Ni-Au-Sn layer has been measured as a function of the aging time for every sample using EDX (Energy Dispersive X-ray analysis) linescans and optical micrographs at 1000X magnification. In addition **Figure 8** features the development of the morphology of this phase from separated-islands.

Figure 9 shows a flower-shaped black phase. This Pb-rich phase, as confirmed by EDX line scans (**Figure 10**), tends to form in all samples. As similar trends were observed in eutectic solder-Cu systems [8], the morphology of this phase could be ascribed to Sn depletion from the eutectic solder.

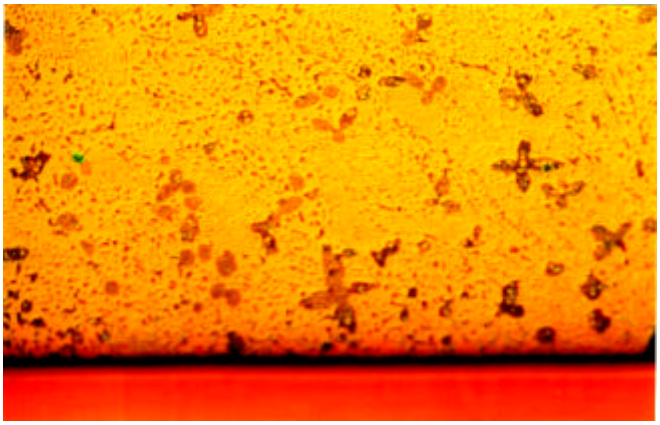

Figure 9: Optical micrograph (1000X)of an electrolytically plated specimen showing the flower-shaped phase.

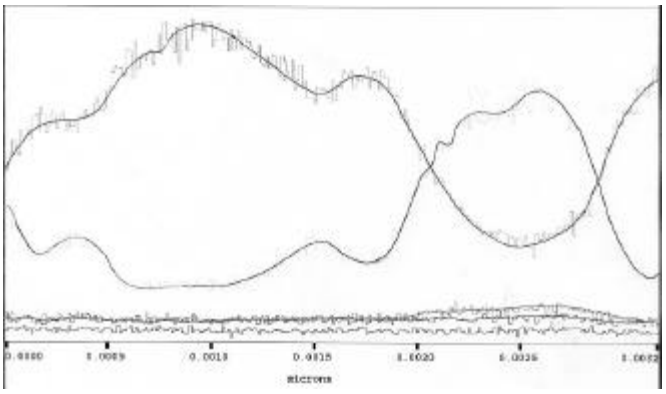

Figure 10: EDX linescan across the flower shaped phase.

EDS maps and linescans acquired from different locations provided the chemical composition of the physically identified phases. As suggested in the equilibrium phase diagram analysis section, Ni_3Sn_4 forms during reflow at the interface. The composition of this phase was determined by x-ray semi-quantitative analysis (ZAF) using a microprobe. The approximate atomic composition of this binary intermetallic according to this analysis is: 44 at% Ni and 56 at% Sn, which is within experimental error of the stoichiometric alloy, Ni_3Sn_4.

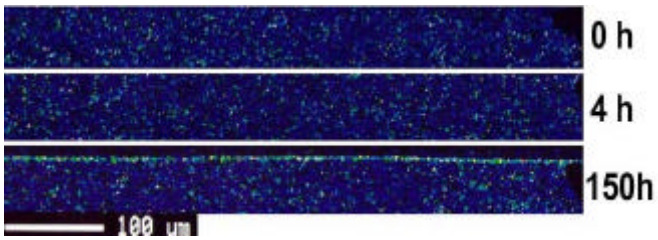

Figure 11: X-ray Au maps acquired from the interface solder-pad metallization for three electrolytic samples respectively unaged, aged 4 h and aged 150 h at 150°C.

As the samples age at 150°C for longer times, Au atoms are able to diffuse appreciable distances throughout the Sn-rich phase of the solder. A combination of energetics and kinetics drives Au atoms to migrate towards the interface solder-Ni_3Sn_4-Ni to form a ternary intermetallic compound $Au_{0.5}Ni_{0.5}Sn_4$, leading the system to increase its stability. **Figure 11** illustrates this mechanism. It shows three x-ray maps belonging to identical samples from a metallurgy standpoint (electrolytic) aged respectively at 0 h (as reflowed), 4 h and 150 h. Au is observed to accumulate at the interface, between the solder and the Ni_3Sn_4 layer. Microchemical analysis inside this phase **Figure 12** revealed the average composition of this compound to be approximately $(Au_{0.5}Ni_{0.5})Sn_4$.

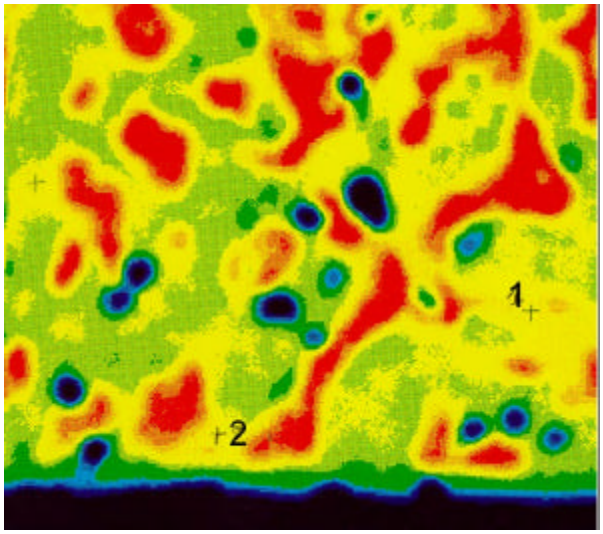

Atomic Ratio:	Group:	
Element:	1	2
P	--	--
Au	8.5387	8.6722
Sn	80.3010	81.0496
Ni	11.1603	10.2782
Total:	100.0000	100.0000

Figure 12: SEM backscattered electrons image of the showing the $(Au_{0.5}Ni_{0.5})Sn_4$ phase at the interface. ZAF analysis at two different spots are included.

Similar trends were observed occasionally in a few of the immersion samples. No Ni-Au-Sn ternary IC growth was noticeable in the case of the selective Au plating, most likely because of the very low initial Au concentration.

III. Effect of intermetallic growth on the mechanical integrity of the joints

Tensile shear tests were undertaken to study the systematics of brittle failure. **Figure 13** displays the test configuration. The BGA packages were diced and cut into solder-ball rows. These rows were attached to a fixture and subjected to compressive stresses using an **INSTRON** tensile-testing machine. The force-displacement curves generated for the tested balls were used to determine the type of failure, the breakage energy and the strength of the joint.

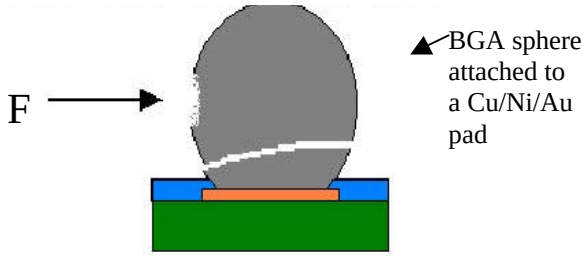

Figure 13: Mechanical test configuration.

Typically joints failed in what was termed to be either a "ductile" or a "brittle" manner. **Figure 14** and **Figure 15** respectively show typical displacement curves of a ductile and a brittle type joint. **Figure 14** belongs to a non-aged specimen while **Figure 15** belongs to a specimen aged for 150 h at 150°C. Ductile fractures were associated with failure in the solder ball, while brittle fractures were assiciated with failure at the Ni/solder interface.

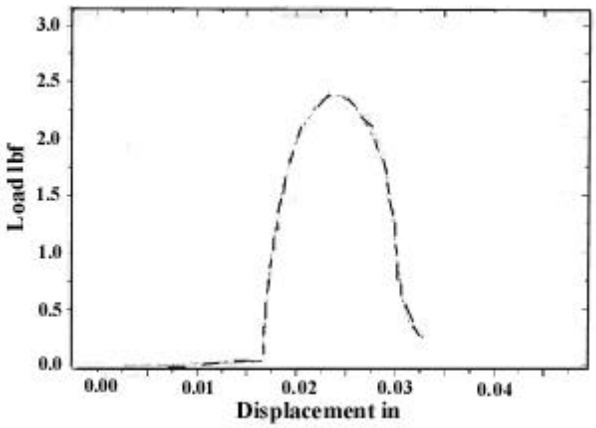

Figure 14: Load-displacement curve for an unaged sample.

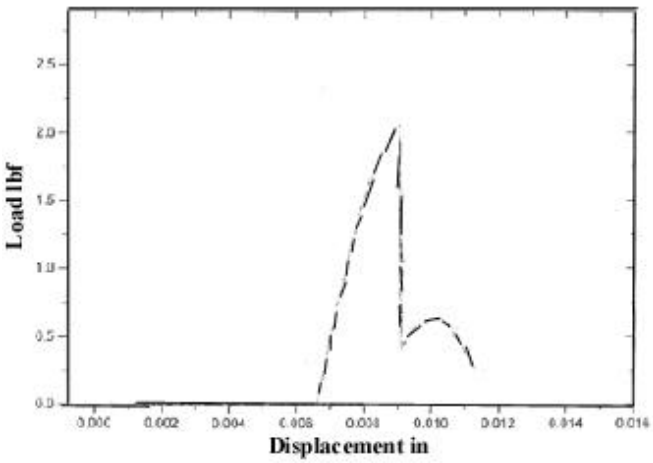

Figure 15: Load-displacement curve for a specimen aged 150 h at 150°C.

The tensile strength of the joint for the unaged samples exceeded that of the aged samples. The drop of joint strength and ductility is perceptible in terms of breakage energy of the joint (the integral of the area under the force-displacement curve). The breakage energy is plotted versus anneal time in **Figure 16**.

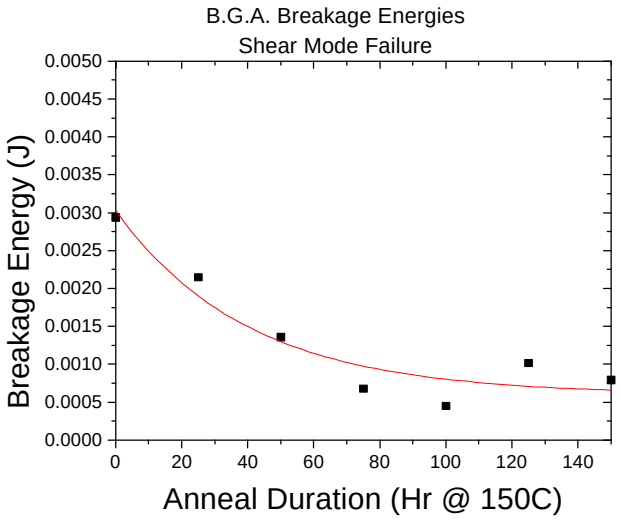

Figure 16: Effect of the annealing time on breakage energy of BGA solder balls.

Observation of the fracture surface of broken electrlytic sample under the microscope reveals a flat surface **Figure 17** which indicates a brittle failure in contrast with a cone-shaped fracture surface **Figure 18** that would correlate with a ductile fracture selective sample.

Figure 17: Optical micrograph (200X) of the fracture surface of an electrolytic sample.

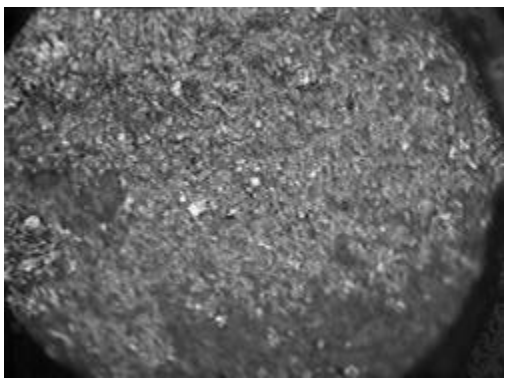

Figure 18: Optical micrograph (200X) of the fracture surface of a selective sample.

Conclusion

A ternary intermetallic phase $(Au_{0.5}Ni_{0.5})Sn_4$ was observed to grow at the Ni_3Sn_4/solder interface upon annealing. This phase grows from the Ni_3Sn_4 binary intermetallic viewed at the interface solder-Ni after solder reflow. The presence of $(Au_{0.5}Ni_{0.5})Sn_4$ decreases the toughness of the joint. The determination of the stoichiometry of the phase $(Au_{0.5}Ni_{0.5})Sn_4$ provides some understanding of why the phase grew at the Ni_3Sn_4/solder interface, as only at this interface were Sn, Au and Ni all readily available.

Acknowledgments

This research was funded the Integrated Electronics Engineering Research Center (IEEC) located in the Watson School at Binghamton University. The IEEC receives funding from the New York State Science and Technology Foundation, the National Science Foundation and a consortium of industrial members.

We gratefully acknowledge discussions with Peter Borgesen, and the use of mechanical testing facilities at Universal Instruments. The Au thickness measurements were provided by Universal Instruments. We thank Ms. Susan Pitely for her efforts in helping us edit and prepare this paper for submission.

References

1. Mei, Z. et al, "Brittle Interfacial Fracture of PBGA Packages Soldered on Electroless Ni/Immersion Au", Hewlett-Packard Company
2. Bader, W. G., "Dissolution of Au, Ag, Pd, Pt, Cu and Ni in a Molten Sn-Lead Solder", *Welding Journal: Research suppliment*, 48(12)(1969) 551s-557s.
3. Kramer, P.A. et al, "The Effect of Low Au Concentrations on the Creep of Eutectic Sn-Lead Joints", *Metallurgical and Materials Transactions A*, Vol.25A, June 1994, pp. 1249-1255.
4. KIM, P.G. et al, "Fast Soldering Reactions On Au Foils", Materials Research Society, *Symposium Proceedings*, Vol.445, 1997, pp.131-136.
5. Ferguson, M. E. et al, "Manufacturing Concerns When Soldering with Au Plated Component Leads or Circuit Board Pads", IE*EE Transactions on Components, Packaging, and Manufacturing Technology-Part C*, Vol. 20, No. 3, July 1997, pp. 186-193.
6. Yost, F.G. et.al., The Mechanics of Solder Alloy Wetting and Spreading, Van Nostrand Reinhold, New York, 1993.
7. Chromik, R. R., "The Thermodynamics and Kinetics of Solid State Reactions In The Pd-Sn System", Masters Thesis SUNY at Binghamton, 1996.
8. Kim, H. K et al, "Morphology of instability of the wetting tips of eutectic SnBi, eutectic Sn-Pb, and pure Sn on Cu", *Materials Research Society*, Vol. 10, No.3, July 1994, pp.497-504.
9. OHRINER, E. K., "Intermetallic Formation in Soldered Copper-Based Alloys at 150°C to 250°C.", *Welding Journal: Research suppliment*, July 1987, pp.191-s/202-s.